4906 J. Med. Chem. 2010, 53, 4906–4916
DOI: 10.1021/jm1002952

Journal of Medicinal Chemistry Article

Diarylaniline Derivatives as a Distinct Class of HIV-1 Non-nucleoside Reverse Transcriptase Inhibitors

Bingjie Qin,[†] Xingkai Jiang,[†] Hong Lu,[§] Xingtao Tian,[†] Florent Barbault,[∥] Li Huang,[⊥] Keduo Qian,[‡] Chin-Ho Chen,[⊥] Rong Huang,[‡] Shibo Jiang,[§] Kuo-Hsiung Lee,[‡] and Lan Xie*,[†]

[†]*Beijing Institute of Pharmacology and Toxicology, 27 Taiping Road, Beijing 100850, China,* [‡]*Natural Products Research Laboratories, University of North Carolina, Chapel Hill, North Carolina 27599,* [§]*Lindsley F. Kimball Research Institute, New York Blood Center, New York, New York 10065,* [∥]*ITODYS, Université Paris Diderot—CNRS UMR 7086, 15 rue Jean de Baif, 75205 Paris, France, and* [⊥]*Duke University Medical Center, Box 2926, Surgical Oncology Research Facility, Durham, North Carolina 27710*

Received March 5, 2010

By using structure-based drug design and isosteric replacement, diarylaniline and 1,5-diarylbenzene-1,2-diamine derivatives were synthesized and evaluated against wild type HIV-1 and drug-resistant viral strains, resulting in the discovery of diarylaniline derivatives as a distinct class of next-generation HIV-1 non-nucleoside reverse transcriptase inhibitor (NNRTI) agents. The most promising compound **37** showed significant EC_{50} values of 0.003−0.032 μM against HIV-1 wild-type strains and of 0.005−0.604 μM against several drug-resistant strains. Current results also revealed important structure−activity relationship (SAR) conclusions for diarylanilines and strongly support our hypothesis that an NH_2 group on the central benzene ring *ortho* to the aniline moiety is crucial for interaction with K101 of the NNRTI binding site in HIV-1 RT, likely by forming H-bonds with K101. Furthermore, molecular modeling studies with molecular mechanism/general Born surface area (MM/GBSA) technology demonstrated the rationality of our hypothesis.

Introduction

According to UNAIDS statistics, more than 60 million people worldwide have been infected by the human immunodeficiency virus (HIV[a]) and about 25 million patients have died of AIDS. In the absence of an effective vaccine, there is a need to develop effective anti-HIV therapeutics to prolong the lives of HIV-infected individuals. Thus far, more than 20 anti-HIV drugs have been approved by the U.S. FDA (www.fda.gov/oashi/aids/virals.html) including reverse transcriptase inhibitors (RTIs), protease inhibitors (PIs), fusion inhibitors, integrase inhibitors, and entry inhibitors (CCR5 coreceptor antagonist). Highly active antiretroviral therapy (HAART), which uses a combination of three to four drugs, can significantly reduce the morbidity and mortality of HIV-1 infected patients. However, as a result of emerging drug-resistant HIV mutants, increasing numbers of HIV-infected patients fail to respond to HAART. Thus, the development of new anti-HIV drugs is urgently required.

To address this need, we have synthesized compounds targeting HIV-1 reverse transcriptase (RT), one of the most important enzymes in the HIV-1 life cycle. It has two known drug-target sites, the substrate binding site and an allosteric site, which is distinct from, but closely located to, the substrate binding site.[1,2] Specifically, we focused on non-nucleoside reverse transcriptase inhibitors (NNRTIs) that interact with the allosteric binding site, a highly hydrophobic cavity, in a non-competitive manner to cause distortion of the three-dimensional structure of the enzyme and thus inhibit RT catalytic function. NNRTIs currently approved for AIDS therapy include nevirapine (**1**), delavirdine (**2**), efavirenz (**3**), and etravirine (TMC125, **4**) (Figure 1).[3] In general, NNRTIs exhibit high inhibitory potency and low toxicity, but drug resistance to NNRTIs has emerged rapidly as a result of mutations in amino acid residues that are in or surround the NNRTI binding site. Compound **4** is the most recently approved NNRTI and is active against many drug-resistant HIV-1 strains. The related riplivirine (TMC278, **5**)[4] is now undergoing phase III clinical trials as a promising new drug candidate. Compounds **4**, **5**, and TMC120 (**6**),[5] a prior clinical candidate, belong to the diarylpyrimidine (DAPY) family (Figure 1) and all are very potent against wild-type and many drug-resistant HIV-1 strains with nanomolar EC_{50} values. They have excellent pharmacological profiles, which has encouraged more research to explore next-generation NNRTI agents.[6−8] In this study, we used isosteric replacements to synthesize new NNRTIs and consequently discovered a series of diarylaniline compounds with high potency against both wild-type and RT-resistant viral strains.

Design

Prior studies[4,9] on DAPY derivatives have resulted in informative SAR conclusions, including (1) a "U" or horseshoe binding conformation in contrast to the typical butterfly like binding shape of **1**−**3**, (2) a proper positioning of two phenyl rings in the eastern and western wings of the NNRT binding pockets, (3) a *para*-substituted aniline moiety in the eastern wing, and (4) two hydrogen bonds between K101 of HIV-1 RT to the NH linker and the nitrogen atom on the pyrimidine

*To whom correspondence should be addressed. Phone/Fax: 86-10-66931690. E-mail: lanxieshi@yahoo.com.

[a] Abbreviations: CC_{50}, concentration for 50% cytotoxicity; DAPY, diarylpyrimidine; EC_{50}, effective concentration for 50% inhibition; HAART, highly active antiretroviral therapy; HIV, human immunodeficiency virus, MM/GBSA, molecular mechanism/general Born surface area; NNRTI, non-nucleoside reverse transcriptase inhibitor; NRTI, nucleoside reverse transcriptase inhibitor; PDB, protein database; PI, protease inhibitor; RF, resistant fold; rmsd, root-mean-square deviation; RT, reverse transcriptase; RTI, reverse transcriptase inhibitor; SAR, structure−activity relationship; SI, selective index (ratio of CC_{50}/EC_{50}).

 Published on Web 06/09/2010

ring.[10] Crystal structures of complexes K103N HIV-1 RT/**4** (protein database (PDB) code: 1sv5), HIV-1 RT/**5** (PDB: 2zd1), K103N/Y181C HIV-1 RT/**5** (PDB: 3bgr), and HIV-1 RT/**6** (PDB: 1s6q)[11,12] further indicate that two flexible linkers between rings allow the inhibitors to adopt bound conformations with either wild-type or mutant HIV-1 RT, resulting in high potency against both wild-type and a wide range of drug-resistant mutant HIV-1 RT. Therefore, the molecular flexibility of DAPY compounds is considered to be very crucial for next-generation NNRTI drugs.

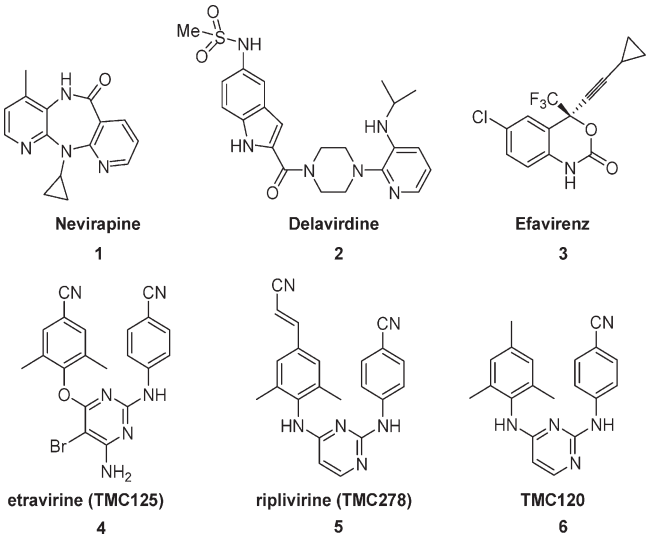

Figure 1. HIV-1 NNRTI agents (**1**−**6**).

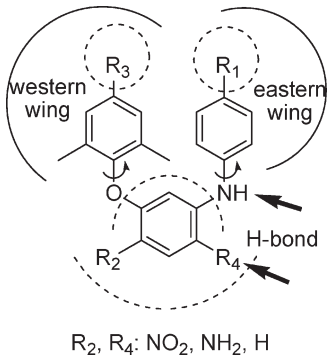

Figure 2. Design of Target Compounds.

On the basis of these SAR data, our strategy was to synthesize new compounds by using isosteric replacement in the central B-ring of DAPY compounds. Unlike the reported DAPY derivatives,[13−15] the new analogues designed in this study (Figure 2) have a central benzene ring rather than the pyrimidine in DAPY compounds. The new compounds also retain two phenyl rings in the eastern and western wings but have different *para*-substituents from the DAPY compounds. Because the presence of a central benzene ring does not change molecular topology and flexibility, these new compounds are expected to have similar binding orientations and conformations to those of DAPYs. However, they will lose the H-bond between K101 and the nitrogen on the pyrimidine ring of DAPY family compounds.[10] To compensate for this loss, we introduced a nitro or amino group (R_4) on the central benzene ring at the *ortho*-position to the aniline ring to serve as H-bond acceptor or donor, respectively, and to interact with K101 on the binding site. Furthermore, we investigated how an additional nitro or amino group (R_2) on the opposite side of the central phenyl ring would affect anti-HIV activity.

Chemistry

All target compounds were synthesized via the short routes detailed in Schemes 1 and 2. The starting material, 1,3-dichloro-4,6-dinitrobenzene or 2,4-dichloro-1-nitrobenzene, is inexpensive and commercially available. The dichloronitrobenzene was reacted with a *para*-substituted aniline in a 1:1.1 molar ratio in DMF at room temperature for less than 40 min in the presence of triethylamine to provide corresponding *N*-aryl-5-chloro- 2,4-dinitroanilines (**7**−**11**) or in the presence of potassium *tert*-butoxide (*t*-BuOK) to provide corresponding *N*-aryl-5-chloro-2-nitroanilines (**12**). The nucleophilic substitution took place between the aromatic amine and the chloride at the *ortho*-position to the nitro group in 71−94% yields. Compounds **7**−**12** were then coupled with a substituted phenol by using microwave irradiation in DMF (or DMSO) in the presence of potassium carbonate with stirring at 190 °C for 15 min to afford diaryl-dinitroanilines (**13**−**23**) and diaryl-mononitroanilines (**24**−**28**).[16,17] Some compounds could also be prepared by the traditional method of heating at 130 °C for 5 h with yields ranging from 74 to 94%. As shown in Scheme 2, dinitro (**19**−**22**) and mononitro (**24**, **26**−**27**) compounds were reduced completely by using hydrazine hydrate in isopropyl alcohol in the presence of $FeCl_3 \cdot 6H_2O$ and activated carbon at reflux for 20−30 min to prepare corresponding diamino (**32**−**35**) or monoamino (**29**−**31**) compounds, respectively, in 83−95% yields . Alternatively, **19**, **21**, and **22** were reduced

Scheme 1. Synthesis of Target Compounds **13**−**28**[a]

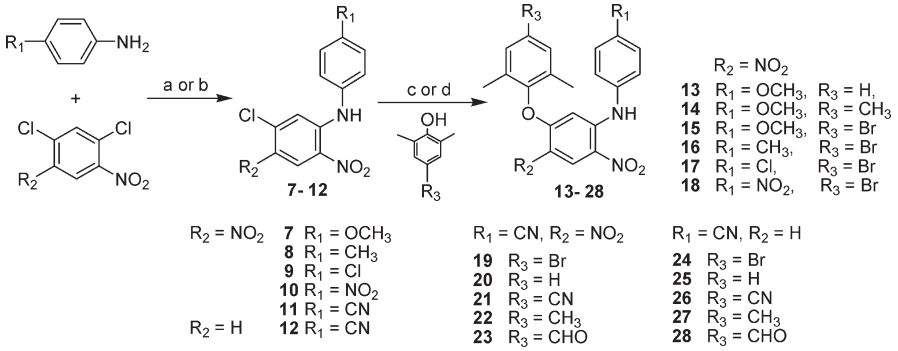

[a] "c or d" indicates two different reaction conditions, the former is under microwave irradiation and the later is a traditional heating method. (a) Et_3N/DMF, rt 40 min; (b) *t*-BuOK/DMF, rt 1 h; (c) K_2CO_3/DMF or DMSO, 190 °C, MW, 10−15 min; (d) K_2CO_3/DMF, 130 °C, 5 h.

Scheme 2[a]

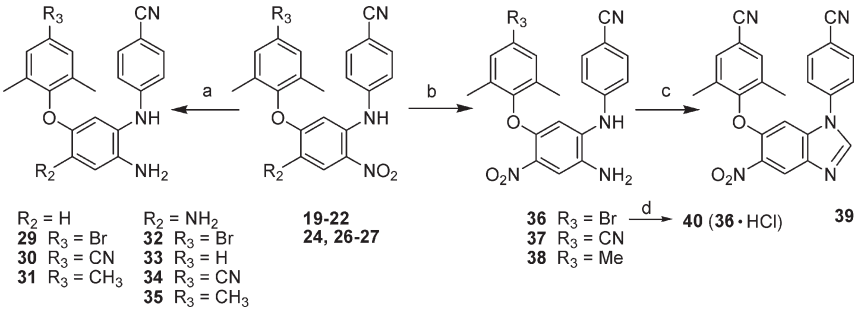

[a] (a) $FeCl_3 \cdot 6H_2O$/C, $N_2H_4 \cdot H_2O$, $(CH_3)_2CHOH$, reflux, 20−30 min; (b) Et_3N/HCOOH, Pd/C, CH_3CN, reflux, 1 h; (c) triethyl orthoformate, HCl (1N in diethyl ether), rt 3 h; (d) CH_3COCH_3, HCl (18% in diethyl ether).

selectively by formic acid in the presence of Pd−C (10%) and triethylamine in acetonitrile under reflux for 1 h to give corresponding 1,5-diaryl-4-nitrobenzene-1,2-diamines **36**−**38**, respectively.[18] Next, **37** was reacted with triethyl orthoformate under acidic conditions to provide the benzoimidazole product **39**. This reaction validated that the nitro group *ortho* to the NH-linked aniline was reduced selectively in the prior step. Furthermore, active compound **36** was converted to hydrochloride salt **40** (shown in Scheme 2) in acetone to investigate the effect of improved molecular water solubility on anti-HIV activity.

Results and Discussion

All target compounds were first tested against wild-type HIV-1 (IIIB strain) replication in the H9 cell line, and the results are summarized in Table 1. The most potent compound **37** had an EC_{50} value of 0.003 μM and an extremely high selective index (SI) of 20887 in this initial assay. Compound **36** and its hydrochloride salt **40** were also very potent, with EC_{50} values of 0.016 and 0.012 μM, respectively; SI values of both compounds were >2800. Other active compounds **27**, **29**−**31**, **34**−**35**, and **38** had EC_{50} values ranging between 0.030 and 0.073 μM and SI values between 520−1698. In addition, compounds **19**, **20**, **22**, **24**, **26**, and **32** showed potency at the submicromolar level and had a SI range of >113−313. These promising results demonstrated that the isosteric replacement of carbon for nitrogen in the central B-ring of DAPY compounds was successful and resulted in the discovery of a series of 1,5-diarylbenzene-1,2-diamine analogues as potent NNRTI agents.

Some SAR results for this compound series can be concluded from the data in Table 1. (1) For the *para*-substituent on the A-ring (R_1 moiety), the cyano (CN) group appears to be necessary at this position for increased anti-HIV activity. Among compounds **13**−**19**, only **19** (R_1 = CN) exhibited high anti-HIV-1 activity with an EC_{50} value of 0.172 μM and SI of >301, while **13**−**18** (R_1 = MeO, Me, Cl, or NO_2) were much less active (EC_{50} >2.99 μM) or inactive. Except for compounds **21**, **23**, **28**, and **33**, all the other compounds containing the active *p*-cyanoanilino A-ring (**19**−**20**, **22**, **24**−**27**, **29**−**32**, **34**−**38**, and **40**) exhibited potent inhibitory activity against wild-type HIV-1 replication. (2) The presence of NH_2 (R_4 moiety) on the central B-ring *ortho* to anilino A-ring position in **29**−**38** and **40** generally enhanced the anti-HIV-1 activity of the analogues (EC_{50}: 0.003−0.161 μM), except for **33**. The NH_2-substituted compounds (**32**, **34**, **35**, **29**, **30**, **31**) were as or more potent than the corresponding NO_2-substituted compounds (**19**, **21**, **22**, **24**, **26**, **27**), respectively. This result is consistent with that in our previous report on diarylpyridine compounds[19] and therefore supports our hypothesis that an amino group at the R_4 position of the central B-ring is crucial for interaction with K101 on the NNRTI binding site and can form additional H-bonds to the protein. (3) On the central B-ring *ortho* to the phenoxy C-ring position (R_2 substituent), NO_2 moiety (**36**−**38**) is more favorable compared with H (**29**−**31**) or NH_2 (**32**, **34**−**35**) for achieving

Table 1. Antiviral and Cytotoxicity Data of **13**−**38** and **40**[a]

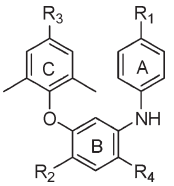

					HIV-1 IIIB in H9 cells		
compd	R_1	R_2	R_3	R_4	EC_{50}[b] (μM)	CC_{50}[c] (μM)	SI[d]
13	OMe	NO_2	H	NO_2	3.840	>61.12	>16
14	OMe	NO_2	Me	NO_2	2.990	>59.10	>20
15	OMe	NO_2	Br	NO_2	3.630	51.23	14
16	Me	NO_2	Br	NO_2	4.310	52.97	12
17	Cl	NO_2	Br	NO_2	NA		
18	NO_2	NO_2	Br	NO_2	>49.7	>49.70	>1
19	CN	NO_2	Br	NO_2	0.172	>51.76	>301
20	CN	NO_2	H	NO_2	0.545	>61.88	>113
21	CN	NO_2	CN	NO_2	4.190	>58.28	>14
22	CN	NO_2	Me	NO_2	0.280	>59.81	>214
23	CN	NO_2	CHO	NO_2	1.530	57.87	38
24	CN	H	Br	NO_2	0.317	>57.08	>180
25	CN	H	H	NO_2	3.147	69.64	22
26	CN	H	CN	NO_2	0.208	>65.10	>313
27	CN	H	Me	NO_2	0.067	>67.02	>1000
28	CN	H	CHO	NO_2	2.190	14.20	6
29	CN	H	Br	NH_2	0.047	44.61	949
30	CN	H	CN	NH_2	0.070	49.77	711
31	CN	H	Me	NH_2	0.073	51.02	699
32	CN	NH_2	Br	NH_2	0.161	38.38	238
33	CN	NH_2	H	NH_2	3.226	53.20	16
34	CN	NH_2	CN	NH_2	0.030	50.95	1698
35	CN	NH_2	Me	NH_2	0.070	50.00	714
36	CN	NO_2	Br	NH_2	0.016	45.47	2,842
37	CN	NO_2	CN	NH_2	0.003	62.66	20887
38	CN	NO_2	Me	NH_2	0.062[e]	32.22[e]	520
40	hydrochloride salt of **36**				0.012	36.42	3,035
AZT					0.052	1873	36019

[a] Assays using H9 cells were performed at Panacos Pharmaceuticals, Inc., Gaithersburg, Maryland. Results are averages of three independent assays. Standard deviations were not provided by Panacos. [b] Concentration of a compound that causes 50% inhibition of HIV-1 IIIB replication. [c] Concentration of a compound that causes cytotoxicity to 50% cells. [d] SI (selective index) = CC_{50}/EC_{50}. [e] Data from Duke University. NA: not active.

Table 2. Data against HIV-1_{IIIB} and Multi-RTI-Resistant Viral Strains[a]

	EC$_{50}$ (μM) in MT-2 cell line				
	wild type	NNRTI-resistant mutant[b]		multi-RTI-resistant mutant[b]	
compd	IIIB	Y181C	A17 (Y181C/K103N)	8605MR	6005MR
34	0.065	1.734	1.244	0.138	0.033
36	0.008	1.298	0.254	0.020	0.007
37	0.005	0.504	0.231	0.005	0.005
1	0.053	> 3.700	> 3.700	> 3.700	> 3.700

[a] Data provided by Panacos Pharmaceuticals Inc.. Results are average of three independent assays. Standard deviations were not provided by Panacos. Compound **1** was used as control due to the fact that **4** was not approved for market at the testing time. [b] NNRTI-resistant mutant and multimutated viral strains were from Panacos Inc. 8605MR: multimutated-RT with M41L, D67N, L210W, T215Y, M184 V, K103N. 6005MR: multimutated-RT with M41L, L74 V, M184 V, L210W, T215Y, ins SS, A98G.

Table 3. Data against HIV-1_{IIIB} and A17 in the MT-2 Cell Line[a]

	EC$_{50}$ (μM) in MT-2 cell line		
compd	IIIB (wild-type)	A17 (Y181C/K103N)[b]	RF
34	0.211 ± 0.053	15.469 ± 9.035	73.3
36	0.052 ± 0.005	1.055 ± 0.088	20.3
37	0.032 ± 0.005	0.604 ± 0.179	18.9
4	0.058 ± 0.001	0.575 ± 0.093	9.9

[a] Data provided by Dr. Shibo Jiang, New York Blood Center. Results are average of three independent assays. [b] The multi-NRTI-resistant strain A17 from NIH with mutations at amino acids 103 (K→N) and 181 (Y→C) in the viral RT domain is highly resistant to NRTIs[21]

high anti-HIV-1 potency. (4) Br, CN, and CH_3 *para*-substituent (R_3 moiety) on the C-ring showed better anti-HIV activity, but CHO and H (**23**, **28**, and **33**) did not. In addition, compound **40**, the hydrochloride salt of **36**, displayed more potent inhibitory activity than **36**, suggesting a possibility to improve water solubility in active compounds.

The most active compounds **34**, **36**, and **37** were further evaluated in comparison with the anti-HIV-1 NNRTI drugs **1** and **4** against wild-type HIV-1 and several RTI-resistant viral strains in the MT-2 cell line. These data are summarized in Tables 2 and 3. As shown in Table 2, we found that both **37** and **36** showed better EC$_{50}$ values (0.005 and 0.008 μM, respectively) against HIV-1_{IIIB} wild-type virus than **1**. While drug **1** lost its antiviral replication activity completely against multi-RTI-resistant mutants, compounds **34**, **36**, and **37** retained their high potency toward these viruses. Impressively, compound **37** still showed the most potent EC$_{50}$ value of 0.005 μM against multi-RTI-resistant mutants 8605MR and 6005MR. Compound **36** also was highly active against these mutants, with similar or slightly lower potency than **37**. Compound **37** kept some of its antiviral activity against NNRTI-resistant mutant Y181C and A17 (Y181C/K103N) with EC$_{50}$ values of 0.504 and 0.231 μM, respectively, while **1** completely lost its potency. Compound **36** also showed moderate inhibition activity toward NNRTI-resistant mutants, although it is less potent than **37**.

The antiviral activity of **34**, **36**, and **37** were further tested against wild-type virus and A17 resistant mutant in parallel with drug **4** after it was approved by US FDA and became available on the market (Table 3). The viral inhibition activity of **37** was slightly better than that of **4** against HIV-1_{IIIB} (wild-type) in this screening, which double-confirmed our results in Table 2. Compounds **37** and **4** showed similar activity (EC$_{50}$: 0.604 and 0.575 μM, respectively) against A17 (from NIH)

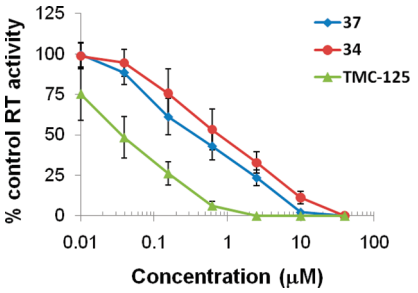

Figure 3. RT inhibition activity of diarylanaline analogues **34** and **37**. Data provided by Dr. Chin-Ho Chen, Duke University Medical Center. Results are average of three independent assays. The RT used in the assays is from HIV-1_{DH012} lysate.

with mutations in the viral RT domain that is highly resistant to NRTIs. These results provide further support that the DAPY pyrimidine ring can be replaced by a benzene ring to generate new potent compounds as a distinct class of next-generation NNRTIs. Meanwhile, although compound **34** ($R_2 = NH_2$) was not as potent as **4** and **37**, it had a higher resistant fold change (RF > 73, ratio of EC$_{50}$ against mutant strain/EC$_{50}$ against wild-type strain) against A17 compared with other compounds, suggesting that the R_2 substituent on the central B-ring may play an important role in the anti-HIV-1 activity against drug-resistant virus.

To confirm RT is the biological target of the newly synthesized diarylaniline analogues, compounds **34** and **37** were evaluated against viral enzyme RT (from HIV-1_{DH012} lysate) and compared with **4**. From Figure 3, we can see all three compounds potently inhibited RT activity. Inhibition of DH012 RT activity by **34** and **37** suggests that HIV-1 RT is a target of the compounds. However, the anti-RT potency of these two compounds was much weaker than **4** even though compound **37** was more potent than **4** against HIV-1 replication (Table 3). The discrepancy in potency between anti-HIV-1 replication and anti-RT activity could be due to the fact that different viral strains were used in the assays. The T cell-adapted virus HIV-1 IIIB was used in the virus replication assay (Table 3), whereas the primary isolate DH012 was used for the RT assay. It is also possible that **34** and **37** inhibited HIV-1 RT in a different manner than **4**. In addition to inhibition of the RNA-dependent DNA polymerase activity of HIV-1 RT, compound **37** might also inhibit DNA-dependent DNA polymerase activity that could not be optimally detected by the RT assay used in this study.

Molecular Modeling Studies

Computational studies of three compounds **21**, **34**, and **37** were carried out to understand how the substituents on the central B-ring of these diarylaniline analogues might interact with HIV-1 RT. Because of the high structural similarity with DAPY, the ligand−protein complexes of the three compounds were created with the help of the experimental crystal structure of HIV-1 in interaction with DAPY compound (PDB: 1s6q).[11]

After energetic optimizations, the ligand positions in the NNRTI binding pocket were carefully checked. To understand the so-called "induced fit effect," all complexes were compared to HIV-RT alone, which was computed by the same protocol. The root mean square deviation (rmsd) permits the determination of geometrical variations between the free and complex protein; all values are compiled

Table 4. RMSD Values of the HIV-1 RT Protein Interacting with **21**, **34**, and **37**, when Compared to the Protein Alone[a]

	rmsd (Å)		
ligand	global	backbone	side-chain
21	0.666	0.501	0.738
34	0.654	0.493	0.725
37	0.635	0.480	0.703

[a] Values are divided into global (all protein atoms), backbone (peptidic bonds), and side-chain (only side-chain atoms).

Table 5. MM/GBSA Energetic Values of the Three Ligand/HIV-1 RT Complexes[a]

	kcal/mol		
energy	ligand **21**	ligand **34**	ligand **37**
Δ*E*elec	31.4	−23.8	−56.5
Δ*E*vdw	−53.8	−61.3	−55.5
Δ*E*int	14.4	7.2	−8.3
Δ*E*gas	−8.0	−77.9	−120.3
Δ*G*solvent_np	−6.2	−6.9	−6.4
Δ*G*solvent_p	1.5	35.3	54.6
Δ*G*solvent	−4.7	28.4	48.2
Δ*G*	−12.7	−49.6	−72.1

[a] *E*elec, *E*vdw, and *E*int signify: electrostatic, van der Waals, and internal (bonds + angles + dihedrals) energies in gas phase (in vacuo), respectively. *E*gas is the sum of the first three energy terms. *G*solvent_p, *G*solvent_np, and *G*solvent are the polar and nonpolar contributions of the solvent free energy, and the sum of these two terms (solvent free energy), respectively; *G* is the free energy of binding (*E*gas + *G*solvent).

in Table 4. From this table, it appears that, globally, the ligand−protein structure is kept and that only small adaptations are made by the protein. Comparison of the backbone and side-chain RMSDs shows that the side-chain residues have moved much more in the optimization process than the peptidic chain, indicating that the secondary enzyme structure was conserved and only small adaptations of residues occurred. In comparison, the less biologically active compound **21** induced more "deformation" (i.e., a higher rmsd) of the protein than either **34** or **37**, denoting that the protein needs a more significant deformation for adaptation to **21**, which is energetically unfavorable for binding.

The molecular mechanics/general Born surface area (MM/GBSA) technique is one of the best computational methods to evaluate free energy of binding, generally from molecular dynamics simulations, for ligands in biological macromolecules.[20,21] Recently, it has been shown on a large number of enzymatic systems (including HIV-1 RT) that the MM/GBSA method is able to rescore docking results, even with only one minimized structure.[22] Therefore, we employed this technique on our three compounds, and the results are compiled in Table 5. To take into account the protein adaptation to the ligands, the calculations were made by considering the three species individually (protein, ligand, and complex). The computed free energies of binding paralleled the experimental antiviral activity data, i.e., the ranking of EC_{50} values. Furthermore, the energetic decompositions indicated which contributions are the most important for the binding affinity and which are not. Comparison of values in Table 5 indicated that the differences of binding free energies come mainly from the gas phase energy and, more precisely, from the electrostatic contribution of the ligand to the protein. However, the nonpolar solvent effect is almost identical for the three compounds. This result may reflect the fact that, in the X-ray structure, the NNRTI binding pocket is deeply inserted into the HIV-1 RT enzyme, and no water molecules are close to the DAPY ligand. Indeed, nonpolar solvent free energy of binding comes from the entropic desolvation of water around the ligand interacting site.

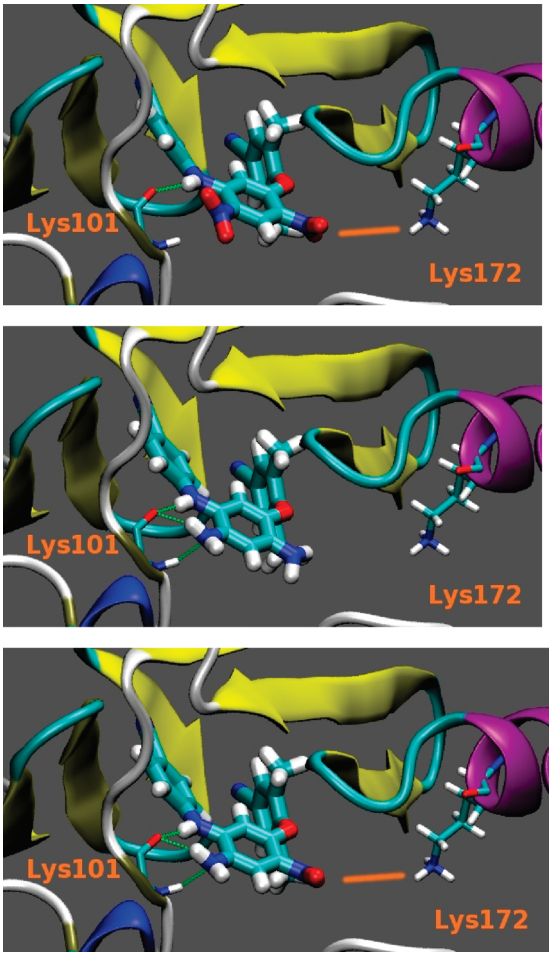

Figure 4. Compounds **21** (top), **34** (middle), and **37** (bottom) in interaction with HIV-1 RT.

On the basis of the above computational studies, the docking of three ligands with HIV-1 RT is illustrated more clearly in Figure 4. Compounds **21**, **34**, and **37** differ structurally only in the identity of the R_2 and R_4 substituents on the central aromatic ring (**21**: NO_2, NO_2; **34**: NH_2, NH_2; **37**: NO_2, NH_2). Therefore, our analyses focused on these moieties. As shown in Figure 4, a hydrogen bond between the NH linker and the peptidic carbonyl oxygen of K101, like that for DAPY compounds, is observed with all three compounds. However, the neighboring amino group (R_4) present in **34** and **37** provides two more hydrogen bonds with K101: one is between the peptidic carbonyl oxygen of the protein residue and one NH vector of the ligand NH_2 group and the second one involves the NH atoms of K101 and targets the nitrogen atom of the ligand NH_2 group. The most active compound **37** also has a nitro group as the R_2 substituent on the central ring. This group provides a small electrostatic interaction with the positively charged K172 (ligand nitrogen−protein nitrogen distance of 6.68 Å; see Figure 3, bottom). When the nitro group in **37** was replaced by an amino group in **34**, the corresponding ligand−protein electrostatic interaction decreased (see Figure 3, middle). Indeed, the distance between the nitrogen atom of the amino moiety of **34** and the K101 nitrogen increased from 6.68 to 7.04 Å, indicating that repulsion has occurred. Moreover, this electrostatic effect was also observed computationally (Table 5) with electrostatic energy values of −56.5 kcal/mol and −23.8 kcal/mol for **37**

and **34**, respectively. In comparison with **34** and **37**, the least active compound **21** has two nitro groups on the central B-ring (see Figure 3, top). Thus, the rightmost (R_2) nitro group of **21** has the same electrostatic interaction with K172 found in **37**, and the ligand nitrogen−protein nitrogen distance shortens to 6.56 Å. However, the presence of the leftmost (R_4) nitro group in **21** completely disrupts the hydrogen bond network with K101. The NH atoms of K101 face the nitrogen atom of the nitro moiety identically as for the amino group, but the nitrogen of a nitro group is electropositive while that of an amino group is electronegative. Thus, for **21**, electrostatic repulsion occurs between the R_4 nitro group and the NH of K101, which is also observed in the computational electrostatic energy value of 31.4 kcal/mol (Table 5). Because a hydrogen bond is mainly electrostatic, the two supplementary H-bonds found with **34** and **37** could explain the experimental EC_{50} differences, which correlated with the computed free energies of binding. Therefore, these molecular modeling results also strongly support our hypothesis and demonstrate why the amino-substituted compounds **29**−**38** are more potent than nitro-substituted compounds **19**−**28**.

Conclusion

On the basis of our isosteric replacement strategy, diarylaniline derivatives were discovered as a distinct class of HIV-1 NNRTI agents. Current results supported our hypothesis that the NH_2 group on the central B-ring *ortho* to the anilino ring position is crucial for interaction with K101 on the NNRTI binding site by forming additional H-bonds. In the series of new compounds, active diarylaniline derivatives are highly potent against both wild-type and drug resistant HIV-1 strains. Among them, the most promising compound is **37** with low EC_{50} values against HIV-1 wild-type (0.003−0.005 μM) and several multidrug-resistant strains (0.005−0.604 μM). Generally speaking, **36** and **37** showed slightly better EC_{50} values (0.052 and 0.032 μM, respectively) than **4** (EC_{50} 0.058 μM), a newly marketed HIV-1 NNRTI drug. In addition, they can be synthesized more conveniently than the DAPY derivatives **4** and **5**.[23,24] The present biological and modeling studies further revealed some important SARs for this series of diarylanilines: (1) the new scaffold can maintain a similar binding orientation and conformation to those of DAPY derivatives, (2) a *para*-cyanoaniline moiety is necessary for anti-HIV activity, (3) an amino group on the central B-ring *ortho* to the aniline moiety position is crucial for achieving high potency, likely by forming H-bonds with K101, (4) an additional nitro group (R_2) on the central aromatic ring is helpful for enhancing affinity of the inhibitor by interaction with K172, and (5) the *para*-substituent (R_3) on the phenoxy ring is changeable but can greatly affect the anti-HIV activity.

Experimental Section

Chemistry. Melting points were measured with an RY-1 melting apparatus without correction. The proton nuclear magnetic resonance (^{1}H NMR) spectra were measured on a JNM-ECA-400 (400 MHz) spectrometer using tetramethylsilane (TMS) as the internal standard. The solvent used was DMSO-d_6 unless otherwise indicated. Mass spectra (MS) were measured on an ABI Perkin-Elmer Sciex API-150 mass spectrometer with electrospray ionization, and the relative intensity of each ion peak is presented as percent (%). The purities of target compounds were ≥95%, measured by HPLC analyses, which were performed by Agilent 1100 HPLC system with a UV detector, using a Grace Alltima HP C18 column (100 mm × 2.1 mm, 3 μm) eluting with a mixture of solvents A and B (condition 1: acetonitrile/water 80:20, flow rate 0.2 mL/min; condition 2: MeOH/water 80:20, flow rate 0.2 mL/min; UV 254 nm). The microwave reactions were performed on a microwave reactor from Biotage, Inc. Thin-layer chromatography (TLC) was performed on silica gel GF_{254} plates. Silica gel GF_{254} (200−300 mesh) from Qingdao Haiyang Chemical Company was used for TLC, preparative TLC, and column chromatography. Medium-pressure column chromatography was performed using a CombiFlash Companion purification system. All chemicals were obtained from Beijing Chemical Works or Sigma-Aldrich, Inc.

General Procedure for the Preparation of N^1-Aryl-5-chloro-2-nitroanilines (7−12). Method A: A *para*-sustituted aniline (1.1 equiv) was added slowly into a solution of 2,4-dichloronitrobenzene (1 equiv) in DMF (3 mL) and triethylamine (1.5 mL, excess). The yellow mixture was stirred at rt for 40 min. The mixture was then poured into water (ca. 30 mL) and stirred for an additional 30 min. The solid product was collected and purified by recrystallization from EtOH. Method B: To a solution of 2,4-dichloronitrobenzene (1 equiv) and a substituted aniline (1.1 equiv) in DMF (3 mL), was slowly added potassium *tert*-butoxide (2 equiv) at ice−water bath temperature, then stirred at rt for about 1 h until the reaction was completed as monitored by TLC. The mixture was poured into ice−water, and pH was adjusted to 6 with 5% aq HCl. The solid was collected, washed with water three times, and purified by recrystallization from EtOH.

5-Chloro-*N*-(4-methoxyphenyl)-2, 4-dinitroaniline (7). Method A, yield 82%, starting with 237 mg (1 mmol) of 1,3-dichloro-4,6-dinitrobenzene and 136 mg (1.1 mmol) of 4-methoxyaniline to afford 226 mg of **7**, yellow solid, mp 150−151 °C. ^{1}H NMR ($CDCl_3$) δ ppm 3.88 (3H, s, OCH_3), 7.03 (2H, d, J = 8.8 Hz, ArH-3′, 5′), 7.05 (1H, s, ArH-6), 7.21 (2H, d, J = 8.8 Hz, ArH-2′, 6′), 9.09 (1H, s, ArH-3), 9.74 (1H, s, NH). MS m/z (%) 324 (M + 1, 100), 326 (M + 3, 30).

5-Chloro-*N*-(4-methylphenyl)-2,4-dinitroaniline (8). Method A, yield 94%, starting with 237 mg (1 mmol) of 1,3-dichloro-4,6-dinitrobenzene and 118 mg (1.1 mmol) of 4-methylaniline to afford 324 mg of **8**, yellow solid, mp 148−150 °C. ^{1}H NMR ($CDCl_3$) δ ppm 2.43 (3H, s, CH_3), 7.12 (1H, s, ArH-6), 7.17 (2H, d, J = 8.0 Hz, ArH-3′, 5′), 7.32 (2H, d, J = 8.0 Hz, ArH-2′, 6′), 9.09 (1H, s, ArH-3), 9.80 (1H, br NH). MS m/z (%): 308 (M + 1, 100), 310 (M + 3, 31).

5-Chloro-*N*-(4-chlorophenyl)-2,4-dinitroaniline (9). Method A, yield 80%, starting with 237 mg (1 mmol) of 1,3-dichloro-4,6-dinitrobenzene and 166 mg (1.3 mmol) of 4-chloroaniline at 80 °C for 20 min to afford 263 mg of **9**, yellow solid, mp 136−138 °C. ^{1}H NMR ($CDCl_3$) δ ppm 7.11 (1H, s, ArH-6), 7.25 (2H, d, J = 8.8 Hz, ArH-3′, 5′), 7.50 (2H, d, J = 8.8 Hz, ArH-2′, 6′), 9.08 (1H, s, ArH-3), 9.77 (1H, s, NH). MS (negative charge) m/z (%): 326 (M − 1, 100), 328 (M + 1, 80).

5-Chloro-*N*-(4-nitrophenyl)-2,4-dinitroaniline (10). Method B, yield 83%, starting with 237 mg (1 mmol) of 1,3-dichloro-4,6-dinitrobenzene and 166 mg (1.2 mmol) of 4-nitroaniline to afford 280 mg of **10**, yellow solid, mp 140−141 °C. ^{1}H NMR δ ppm 7.55 (1H, s, ArH-6), 7.60 (2H, d, J = 8.8 Hz, ArH-2′, 6′), 8.29 (2H, d, J = 8.8 Hz, ArH-3′, 5′), 8.90 (1H, s, ArH-3), 10.19 (1H, s, NH). MS m/z (%): 308 (M + 1, 100), 310 (M + 3, 30).

5-Chloro-*N*-(4-cyanophenyl)-2,4-dinitroaniline (11). Method B, yield 89%, starting with 237 mg (1 mmol) of 1,3-dichloro-4,6-dinitrobenzene and 130 mg (1.1 mmol) of 4-cyanoaniline to afford 284 mg of **11**, yellow solid, mp 174−176 °C. ^{1}H NMR ($CDCl_3$) δ ppm 7.41 (1H, s, ArH-6), 7.57 (2H, d, J = 8.8 Hz, ArH-2′, 6′), 7.91 (2H, d, J = 8.8 Hz, ArH-3′, 5′), 8.90 (1H, s, ArH-3), 10.07 (1H, s, NH). MS m/z (%): 319 (M + 1, 100), 321 (M + 3, 23).

5-Chloro-*N*-(4-cyanophenyl)-2-nitroaniline (12). Method B, yield 71%, starting with 576 mg (3 mmol) of 2,4-dichloro-1-nitrobenzene and 425 mg (3.6 mmol) of 4-cyanoaniline to afford 583 mg of **12**, red−yellow solid, mp 123−124 °C. ^{1}H NMR δ ppm 7.17 (1H, d, J = 9.0 Hz, ArH-4), 7.40 (2H, d, J = 8.8 Hz,

ArH-2′, 6′), 7.45 (1H, s, ArH-6), 7.78 (2H, d, J = 8.8 Hz, ArH-3′, 5′), 8.14 (1H, d, J = 9.0 Hz, ArH-3), 9.48 (1H, s, NH). MS m/z (%): 272 (M − 1, 100), 321 (M + 1, 22).

General Preparation of Diphenylether (13−28). Method C (microwave): A mixture of *N*-aryl-5-chloro-2-nitroaniline (1 equiv) and 2,6-dimethylphenol (1.2 equiv) in DMF (3 mL) in the presence of anhydrous potassium carbonate (2 equiv) was irradiated under microwave with stirring at 190 °C for 15 min. The mixture was poured into ice−water, pH adjusted to neutral with 5% HCl aq, and the mixture extracted with EtOAc three times. After removal of organic solvent in vacuo, crude product was purified by PTLC or a silica column (eluent: petroleum ether/EtOAc). Method D (traditional): A mixture of *N*-aryl-5-chloro-2-nitroaniline (**11** or **12**, 1 equiv) and a *para*-substituted 2,6-dimethylphenol (1.2 equiv) in DMF in the presence of anhydrous potassium carbonate (excess) was heated at 130 °C for 5 h. Workup was the same as above, and crude product was purified by a silica gel column.

5-(2″,6″-Dimethylphenoxy)-*N*-(4′-methoxyphenyl)-2,4-dinitroaniline (13). Method C, yield 75%, starting with 129 mg (0.4 mmol) of **7** and 59 mg (0.48 mmol) of 2,6-dimethylphenol to afford 123 mg of **13**, yellow solid, mp 169−170 °C. ^{1}H NMR ($CDCl_3$) δ ppm 2.06 (6H, s, 2 × CH_3), 3.78 (3H, s, OCH_3), 5.91 (1H, s, ArH-6), 6.75 (2H, d, J = 8.8 Hz, ArH-2′, 6′), 6.89 (2H, d, J = 8.8 Hz, ArH-3′, 5′), 7.11 (1H, t, J = 6.8 Hz, ArH-4″), 7.69 (2H, d, J = 6.8 Hz, ArH-3″, 5″), 8.96 (1H, s, ArH-3), 9.70 (1H, s, NH). MS m/z (%): 410 (M + 1, 100). HPLC purity: 99.4%.

***N*^{1}-(4′-Methoxyphenyl)-5-(2″,4″,6″-trimethylphenoxy)-2,4-dinitroaniline (14).** Method C, yield 33%, starting with 162 mg (0.5 mmol) of **7** and 82 mg (0.6 mmol) of 2,4,6-trimethylphenol to afford 70 mg of **14**, red solid, mp 155−158 °C. ^{1}H NMR ($CDCl_3$) δ ppm 1.98 (6H, s, 2 × CH_3), 2.16 (3H, s, CH_3), 3.73 (3H, s, OCH_3), 5.82 (1H, s, ArH-6), 6.69 (2H, s, ArH), 6.72 (2H, d, J = 8.8 Hz, ArH-2′, 6′), 6.84 (2H, d, J = 8.8 Hz, ArH-3′, 5′), 9.11 (1H, s, ArH-3), 9.60 (1H, s, NH). MS m/z (%): 424 (M + 1, 100). HPLC purity: 98.3%.

5-(4″-Bromo-2″,6″-dimethylphenoxy)-*N*-(4′-methoxyphenyl)-2,4-dinitroaniline (15). Method C, yield 53%, starting with 647 mg (2 mmol) of **7** and 422 mg (2.1 mmol) of 4-bromo-2,6-dimethylphenol to afford 517 mg of **15**, yellow solid, mp 221−223 °C. ^{1}H NMR ($CDCl_3$) δ ppm 2.07 (6H, s, 2 × CH_3), 3.78 (3H, s, OCH_3), 5.91 (1H, s, ArH-6), 6.75 (2H, d, J = 9.0 Hz, ArH-2′, 6′), 6.89 (2H, d, J = 9.0 Hz, ArH-3′, 5′), 7.34 (2H, s, ArH-3″, 5″), 9.17 (1H, s, ArH-3), 9.68 (1H, s, NH). MS m/z (%): 488 (M + 1, 100), 490 (M + 3, 98). HPLC purity: 95.8%.

5-(4″-Bromo-2″,6″-dimethylphenoxy)-*N*-(4′-methylphenyl)-2,4-dinitroaniline (16). Method C, yield 52%, starting with 154 mg (0.5 mmol) of **8** and 121 mg (0.6 mmol) of 4-bromo-2,6-dimethylphenol to afford 123 mg of **16**, yellow solid, mp 200−202 °C. ^{1}H NMR ($CDCl_3$) δ ppm 2.08 (6H, s, 2 × CH_3), 2.36 (3H, s, CH_3), 5.89 (1H, s, ArH-6), 6.86 (2H, d, J = 8.8 Hz, ArH-3′, 5′), 7.10 (2H, d, J = 8.8 Hz, ArH-2′, 6′), 7.16 (2H, s, ArH-3″, 5″), 9.17 (1H, s, ArH-3), 9.71 (1H, s, NH). MS m/z (%): 472 (M + 1, 100), 474 (M + 3, 92). HPLC purity: 97.5%.

5-(4″-Bromo-2″,6″-dimethylphenoxy)-*N*-(4′-chlorophenyl)-2,4-dinitroaniline (17). Method C, yield 64%, starting with 328 mg (1.0 mmol) of **9** and 201 mg (1.0 mmol) of 4-bromo-2,6-dimethylphenol to afford 315 mg of **17**, yellow solid, mp 206−208 °C. ^{1}H NMR δ ppm 2.01 (6H, s, 2 × CH_3), 5.70 (1H, s, ArH-6), 7.15 (2H, d, J = 8.8 Hz, ArH-3′, 5′), 7.35 (2H, d, J = 8.8 Hz, ArH-2′, 6′), 7.37 (2H, s, ArH-3″, 5″), 8.96 (1H, s, ArH-3), 10.01 (1H, s, NH). MS m/z (%): 492 (M + 1, 70), 494 (M + 3, 100). HPLC purity: 96.3%.

5-(4″-Bromo-2″,6″-dimethylphenoxy)-*N*-(4′-nitrophenyl)-2,4-dinitroaniline (18). Method C, yield 78%, starting with 154 mg (0.44 mmol) of **10** and 107 mg (0.53 mmol) of 4-bromo-2,6-dimethylphenol to afford 173 mg of **18**, yellow solid, mp 190−191 °C. ^{1}H NMR δ ppm 2.05 (6H, s, 2 × CH_3), 6.06 (1H, s, ArH-6), 7.31 (2H, d, J = 8.8 Hz, ArH-2′, 6′), 7.41 (2H, s, ArH-3″, 5″), 8.13 (2H, d, J = 8.8 Hz, ArH-3′, 5′), 8.96 (1H, s, ArH-3), 10.13 (1H, s, NH). MS m/z (%): 503 (M + 1, 100), 505 (M + 3, 98). HPLC purity: 97.7%.

5-(4″-Bromo-2″,6″-dimethylphenoxy)-*N*-(4′-cyanophenyl)-2,4-dinitroaniline (19). Method D, yield 85%, starting with 3.18 g (10 mmol) of **11** and 2.4 g (12 mmol) of 2,6-dimethyl-4-bromophenol in the presence of K_2CO_3 (excess, 3.0 g, 21.7 mmol) to afford 4.3 g of **19**, yellow solid, mp 276−278 °C. ^{1}H NMR δ ppm 2.05 (6H, s, 2 × CH_3), 5.93 (1H, s, ArH-6), 7.28 (2H, d, J = 8.8 Hz, ArH-2′, 6′), 7.42 (2H, s, ArH-3″, 5″), 7.73 (2H, d, J = 8.8 Hz, ArH-3′, 5′), 8.96 (1H, s, ArH-3), 10.07 (1H, s, NH). MS (negative charge) m/z (%): 481 (M − 1, 100), 483 (M + 1, 99). HPLC purity: 98.5%.

***N*-(4′-Cyanophenyl)-5-(2″,6″-dimethylphenoxy)-2,4-dinitroaniline (20).** Method C, yield 81%, starting with 319 mg (1.0 mmol) of **11** and 146.4 mg (1.2 mmol) of 2,6-dimethylphenol to afford 327 mg of **20**, orange solid, mp 229−230 °C. ^{1}H NMR δ ppm 2.06 (6H, s, 2 × CH_3), 6.01 (1H, s, ArH-6), 7.09 (2H, d, J = 8.8 Hz, ArH-2′, 6′), 7.11 (1H, t, J = 6.8 Hz, ArH-4″), 7.28 (2H, d, J = 8.8 Hz, ArH-3′, 5′), 7.69 (2H, d, J = 6.8 Hz, ArH-3″, 5″), 8.96 (1H, s, ArH-3), 10.07 (1H, s, NH). MS m/z (%): 405 (M + 1, 100); HPLC purity: 99.9%.

5-(4″-Cyano-2″,6″-dimethylphenoxy)-*N*-(4′-cyanophenyl)-2,4-dinitroaniline (21). Method D, yield 94%, starting with 1.27 g (4.0 mmol) of **11** and 705 mg (4.8 mmol) of 2,6-dimethyl-4-cyanophenol in DMF (4 mL) in the presence of anhydrous potassium carbonate (966 mg, 7 mmol) to afford 1.61 g of **21**, orange solid, mp > 300 °C. ^{1}H NMR δ ppm 2.08 (6H, s, 2 × CH_3), 5.90 (1H, s, ArH-6), 7.29 (2H, d, J = 8.8 Hz, ArH-2′, 6′), 7.73 (2H, s, ArH-3″, 5″), 7.74 (2H, d, J = 8.8 Hz, ArH-3′, 5′), 8.97 (1H, s, ArH-3), 10.07 (1H, s, NH). MS m/z (%): 430 (M + 1, 100). HPLC purity: 98.1%.

***N*-(4′-Cyanophenyl)-2,4-dinitro-5-(2″,4″,6″-trimethylphenoxy)-aniline (22).** Method C, yield 70%, starting with 637 mg (2 mmol) of **11** and 286 mg (2.1 mmol) of 2,4,6-trimethylphenol to afford 580 mg of **22**, yellow solid, mp 223−225 °C. ^{1}H NMR δ ppm 2.00 (6H, s, 2 × CH_3), 2.22 (3H, s, CH_3), 5.92 (1H, s, ArH-6), 6.95 (2H, s, ArH-3″, 5″), 7.27 (2H, d, J = 8.8 Hz, ArH-2′, 6′), 7.72 (2H, d, J = 8.8 Hz, ArH-3′, 5′), 8.95 (1H, s, ArH-3), 10.04 (1H, s, NH). MS m/z (%): 419 (M + 1, 100). HPLC purity: 98.3%.

***N*-(4′-Cyanophenyl)-5-(2″,6″-dimethyl-4″-formylphenoxy)-2,4-dinitroaniline (23).** Method C, yield 74%, starting with 160 mg (0.5 mmol) of **11** and 113 mg (0.6 mmol) 4-hydroxy-3,5-dimethylbenzaldehyde to afford 144 mg of **23**, yellow solid, mp 260−263 °C. ^{1}H NMR ($CDCl_3$) δ ppm 2.23 (6H, s, 2 × CH_3), 6.24 (1H, s, ArH-6), 7.10 (2H, d, J = 8.8 Hz, ArH-2′, 6′), 7.54 (2H, d, J = 8.8 Hz, ArH-3′, 5′), 7.67 (2H, s, ArH-3″, 5″), 9.20 (1H, s, ArH-3), 9.97 (2H, s, NH and CHO). MS m/z (%) 433 (M + 1, 100). HPLC purity: 98.7%.

5-(4″-Bromo-2″,6″-dimethylphenoxy)-*N*-(4′-cyanophenyl)-2-nitroaniline (24). Method C, yield 93%, starting with **12** (100 mg, 0.36 mmol) and potassium 4-bromo-2,6-dimethylphenoxide (105 mg, 0.44 mmol) in DMF (2 mL) were irradiated under microwave with stirring at 192 °C for 10 min to get 147 mg of **24**, light-yellow solid, mp 143 °C. ^{1}H NMR ($CDCl_3$) δ ppm 2.03 (6H, s, 2 × CH_3), 6.19 (1H, dd, J = 9.2 and 2.4 Hz, ArH-6), 6.74 (1H, d, J = 2.4 Hz, ArH-4), 7.21 (2H, d, J = 8.8 Hz, ArH-2′, 6′), 7.30 (2H, s, ArH-3″, 5″), 7.57 (2H, d, J = 8.8 Hz, ArH-3′, 5′), 8.13 (1H, d, J = 9.2 Hz, ArH-3), 9.69 (1H, s, NH). MS m/z (%): 438 (M + 1, 100), 440 (M + 3, 98). HPLC purity: 95.7%.

***N*-(4′-Cyanophenyl)-5-(2″,6″-dimethylphenoxy)-2-nitroaniline (25).** Method C, yield 31%, starting with **12** (50 mg, 0.18 mmol) and 2,6-dimethylphenol (31 mg, 0.25 mmol) in the presence of potassium carbonate (58 mg, 0.42 mmol) in DMSO (2 mL) to afford 20 mg of **25**, yellow solid, mp 158−60 °C. ^{1}H NMR ($CDCl_3$) δ ppm 2.12 (6H, s, 2 × CH_3), 6.35 (1H, q, J_1 = 9.2 Hz, J_2 = 2.4 Hz, ArH-4), 6.73 (1H, d, J = 2.4 Hz, ArH-6), 7.10 (3H, m, ArH-3″, 4″, 5″), 7.24 (2H, d, J = 8.4 Hz, ArH-2′, 6′), 7.59 (2H, d, J = 8.4 Hz, ArH-3′, 5′), 8.21 (1H, d, J = 9.2 Hz, ArH-3), 9.76 (1H, s, NH). MS m/z (%): 360 (M^+, 100). HPLC purity: 96.6%.

5-(4″-Cyano-2″,6″-dimethylphenoxy)-*N*-(4′-cyanophenyl)-2-nitroaniline (26). Method D, yield 79%, starting with 821 mg (3 mmol) of **12** and 530 mg (3.6 mmol) of 2,6-dimethyl-4-cyanophenol in the presence of K_2CO_3 (excess, 1.45 g, 10.5 mmol) to afford 0.92 g of **26**, yellow solid, mp186−188 °C. ^{1}H NMR ($CDCl_3$) δ ppm 2.16 (6H, s, 2 × CH_3), 6.15 (1H, dd, J = 9.2 and 2.4 Hz, ArH-4), 6.87 (1H, d, J = 2.4 Hz, ArH-6), 7.31 (2H, d, J = 8.8 Hz, ArH-2′, 6′), 7.45 (2H, s, ArH-3″, 5″), 7.66 (2H, d, J = 8.8 Hz, ArH-3′, 5′), 8.21 (1H, d, J = 9.2 Hz, ArH-3), 9.75 (1H, s, NH). MS m/z (%): 385 (M + 1, 100). HPLC purity: 99.0%.

***N*-(4′-Cyanophenyl)-5-(2″,4″,6″-trimethylphenoxy)-2-nitroaniline (27).** Method D, yield 74%, starting with 274 mg (1 mmol) of **12** and 241 mg (1.2 mmol) of 2,4,6-trimethylphenol in the presence of excess K_2CO_3 to afford 225 mg of **27**, yellow solid, mp 168−170 °C. ^{1}H NMR ($CDCl_3$) δ ppm 2.00 (6H, s, 2 × CH_3), 2.23 (3H, s, CH_3), 6.25 (1H, d, J = 9.2 Hz, ArH-4), 6.69 (1H, s, ArH-6), 6.84 (2H, s, ArH-3″, 5″), 7.18 (2H, d, J = 8.8 Hz, ArH-2′, 6′), 7.53 (2H, d, J = 8.8 Hz, ArH-3′, 5′), 8.12 (1H, d, J = 9.2 Hz, ArH-3), 9.67 (1H, s, NH). MS m/z (%) 474 (M + 1, 100). HPLC purity: 95.9%.

***N*-(4′-Cyanophenyl)-5-(2″,6″-dimethyl-4″-formylphenoxy)-2-nitroaniline (28).** Method C, yield 70%, starting with 137 mg (0.5 mmol) of **12** and 90 mg (0.6 mmol) of 4-hydroxy-3,5- dimethylbenzaldehyde to afford 135 mg of **28**, yellow solid, mp 152−155 °C. ^{1}H NMR ($CDCl_3$) δ ppm 2.21 (6H, s, 2 × CH_3), 6.23 (1H, dd, J = 8.8 and 2.4 Hz, ArH-4), 6.84 (1H, d, J = 2.4 Hz, ArH-6), 7.30 (2H, d, J = 8.8 Hz, ArH-2′, 6′), 7.64 (2H, d, J = 8.8 Hz, ArH-3′, 5′), 7.67 (2H, s, ArH), 8.22 (1H, d, J = 8.8 Hz, ArH-3), 9.76 (1H, br s, NH), 9.97 (1H, s, CHO). MS m/z (%): 338 (M + 1, 100). HPLC purity: 98.6%.

General Preparation of 1,5-Diarylbenzene-1,2-diamines or 1,2,4-Triamines (29−38). To a solution of a diaryl-nitrobenzene (**24**, **26**−**27**, or **19**−**22**, 1 equiv) in 15 mL of isopropyl alcohol was added $FeCl_3 \cdot 6H_2O$ (1 equiv), activated carbon (2 equiv), and $N_2H_4 \cdot H_2O$ (10 equiv), successively. The mixture was refluxed for 20−30 min. After removal of carbon and solvent, the residue was purified by a silica gel column (eluent: $CHCl_3$/MeOH 40:1) to obtain corresponding diarylbenzene-1,2-diamine or -1,2,4-triamines, respectively.

5-(4″-Bromo-2″,6″-dimethylphenoxy)-*N*^{1}-(4′-cyanophenyl)benzene-1,2-diamine (29). Yield 83%, starting with 150 mg (0.34 mmol) of **24** to afford 115 mg of **29**, brown solid, mp 154−155 °C. ^{1}H NMR δ ppm 2.07 (6H, s, 2 × CH_3), 4.55 (2H, s, $ArNH_2$), 6.34 (1H, s, ArH-6), 6.47 (1H, d, J = 8.8 Hz, ArH-4), 6.65 (2H, d, J = 8.8 Hz, ArH-2′, 6′), 6.73 (1H, d, J = 8.8 Hz, ArH-3), 7.34 (2H, s, ArH-3″, 5″), 7.49 (2H, d, J = 8.8 Hz, ArH-3′, 5′), 8.08 (1H, s, NH). MS m/z (%) 408 (M + 1, 100), 410 (M + 3, 98). HPLC purity: 96.8%.

5-(4″-Cyano-2″,6″-dimethylphenoxy)-*N*^{1}-(4′-cyanophenyl)benzene-1,2-diamine (30). Yield 83%, starting with 130 mg (0.34 mmol) of **26** to afford 100 mg of **30**, brown solid, mp 154−156 °C. ^{1}H NMR ($CDCl_3$) δ ppm 2.18 (6H, s, 2×CH_3), 3.0−4.0 (2H, NH_2), 5.67 (1H, s, NH), 6.47 (1H, q, J = 8.8 and 2.8 Hz, ArH-4), 6.58 (1H, d, J = 2.8 Hz, ArH-6), 6.70 (2H, d, J = 8.8 Hz, ArH-2′, 6′), 6.74 (1H, d, J = 8.8 Hz, ArH-3), 7.40 (2H, s, ArH-3″, 5″), 7.47 (2H, d, J = 8.8 Hz, ArH-3′, 5′). MS m/z (%): 355 (M + 1, 100). HPLC purity: 99.2%.

***N*^{1}-(4′-Cyanophenyl)-5-(2″,4″,6″-trimethylphenoxy)benzene-1,2-diamine (31).** Yield 84%, starting with 150 mg (0.4 mmol) of **27** to afford 116 mg of **31**, mp152−154 °C. ^{1}H NMR δ ppm 2.02 (6H, s, 2 × CH_3), 2.22 (3H, s, CH_3), 4.48 (2H, s, NH_2), 6.29 (1H, d, J = 2.8 Hz, ArH-6), 6.48 (1H, dd, J = 8.4 and 2.8 Hz, ArH-4), 6.64 (1H, d, J = 8.4 Hz, ArH-3), 6.72 (2H, d, J = 8.8 Hz, ArH-2′, 6′), 7.48 (2H, d, J = 8.8 Hz, ArH-3′, 5′), 8.07 (1H, s, NH). MS m/z (%): 344 (M + 1, 100). HPLC purity: 99.8%.

5-(4″-Bromo-2″,6″-dimethylphenoxy)-*N*^{1}-(4′-cyanophenyl)benzene-1,2,4-triamine (32). Yield 95%, starting with 150 mg (0.31 mmol) of **19** to afford 125 mg of **32**, brown solid, mp 181−183 °C. ^{1}H NMR δ ppm 2.08 (6H, s, 2×CH_3), 4.28 (2H, s, NH_2), 4.91 (2H, s, NH_2), 5.70 (1H, s, ArH-3), 6.22 (1H, s, ArH-6), 6.43 (2H, d, J = 8.8 Hz, ArH-2′, 6′), 7.30 (2H, s, ArH-3″, 5″), 7.38 (2H, d, J = 8.8 Hz, ArH-3′, 5′), 7.71 (1H, s, NH). MS m/z (%): 423 (M + 1, 100), 425 (M + 3, 98). HPLC purity: 96.1%.

***N*^{1}-(4′-Cyanophenyl)-5-(2″,6″-dimethylphenoxy)benzene-1,2,4-triamine (33).** Yield 30%, starting with 152 mg (0.31 mmol) of **20** to afford 39 mg of **33**, brown solid, mp 156−158 °C. ^{1}H NMR δ ppm 2.08 (6H, s, 2 × CH_3), 4.22 (2H, s, NH_2-4), 4.84 (2H,s, NH_2-2), 5.70 (1H, s, ArH-3), 6.23 (1H, s, ArH-6), 6.43 (2H, d, J = 8.8 Hz, ArH-2′, 6′), 6.99 (2H, d, J = 6.8 Hz, ArH-3″, 5″), 7.07 (1H, t, J = 6.8 Hz, ArH-4″), 7.36 (2H, d, J = 8.8 Hz, ArH-3′, 5′), 7.67 (1H, s, NH). MS m/z (%): 345 (M^+, 100). HPLC purity: 99.6%.

5-(4″-Cyano-2″,6″-dimethylphenoxy)-*N*^{1}-(4′-cyanophenyl)benzene-1,2,4-triamine (34). Yield 86%, starting with 300 mg (0.7 mmol) of **21** to afford 223 mg of **34**, brown solid, mp 144 °C. ^{1}H NMR δ ppm 2.08 (6H, s, 2 × CH_3), 4.33 (2H, s, NH_2), 4.97 (2H, s, NH_2), 5.71 (1H, s, ArH-3), 6.23 (1H, s, ArH-6), 6.43 (2H, d, J = 8.8 Hz, ArH-2′, 6′), 7.38 (2H, d, J = 8.8 Hz, ArH-3′, 5′), 7.61 (2H, s, ArH-3″, 5″), 7.71 (1H, s, NH). MS m/z (%) 370 (M + 1, 100). HPLC purity: 100.0%.

***N*^{1}-(4′-Cyanophenyl)-5-(2″,4″,6″-trimethylphenoxy)benzene-1,2,4-triamine (35).** Yield 85%, starting with 150 mg (0.36 mmol) of **22** to afford 110 mg of **35**, light-brown solid, mp 152−154 °C. ^{1}H NMR ($CDCl_3$) δ ppm 2.08 (6H, s, 2 × CH_3), 2.26 (3H, s, CH_3), 3.50 (2H, s, NH_2), 4.0 (2H, s, NH_2), 5.33 (1H, s, ArH-6), 5.97 (1H, s, ArH-3), 6.29 (1H, s, NH), 6.47 (2H, d, J = 8.8 Hz, ArH-2′, 6′), 6.86 (2H, s, ArH-3″, 5″), 7.36 (2H, d, J = 8.8 Hz, ArH-3′, 5′). MS m/z (%): 359 (M + 1, 100). HPLC purity: 100.0%.

5-(4″-Bromo-2″,6″-dimethylphenoxy)-*N*^{1}-(4′-cyanophenyl)-4-nitrobenzene-1,2-diamine (36). Pd−C (10%, 30 mg) was added to a solution of **19** (338 mg, 0.7 mmol) in acetonitrile (6 mL) and triethylamine (6 mL). The mixture was cooled to −15 °C, and then formic acid (95%, 1 mL, excess) in acetonitrile (4 mL) was slowly added at the low temperature. The mixture was then heated to reflux for 1 h, following which the Pd−C and solvent were removed. The residue was purified by PTLC (petroleum ether/EtOAc 4:1) to obtain 269 mg of **36**, yield 85%, deep-red solid, mp 218−220 °C. ^{1}H NMR δ ppm 2.07 (6H, s, 2 × CH_3), 5.13 (2H, s, NH_2), 6.16 (1H, s, ArH-6), 6.82 (2H, d, J = 8.4 Hz, ArH-2′, 6′), 7.40 (2H, s, ArH-3″, 5″), 7.55 (2H, d, J = 8.4 Hz, ArH-3′, 5′), 7.95 (1H, s, ArH-3), 8.45 (1H, s, NH). MS m/z (%) 453 (M + 1, 95), 455 (M + 3, 100). HPLC purity: 97.0%.

5-(4″-Cyano-2″,6″-dimethylphenoxy)-*N*^{1}-(4′-cyanophenyl)-4-nitrobenzene-1,2-diamine (37). The preparation was the same as that of **36**. Yield 86%, starting with 150 mg (0.35 mmol) of **21** to afford 237 mg of **37**, red solid, mp 224−226 °C. ^{1}H NMR δ ppm 2.07 (6H, s, 2 × CH_3), 5.17 (2H, s, NH_2), 6.15 (1H, s, ArH-6), 6.81 (2H, d, J = 8.8 Hz, ArH-2′, 6′), 7.55 (2H, d, J = 8.8 Hz, ArH-3′, 5′), 7.71 (2H, s, ArH), 8.06 (1H, s, ArH-3), 8.45 (1H, s, NH). MS m/z (%): 400 (M + 1, 100). HPLC purity: 96.8%.

***N*^{1}-(4′-Cyanophenyl)-5-(2″,4″,6″-trimethylphenoxy)-4-nitrobenzene-1,2-diamine (38).** The preparation was the same as that of **36**. Yield 79%, starting with 300 mg (0.72 mmol) of **22** to afford 220 mg of **38**, red solid, mp 110−112 °C. ^{1}H NMR ($CDCl_3$) δ ppm 2.07 (6H, s, 2 × CH_3), 2.28 (3H, s, CH_3), 6.36 (1H, s, ArH-6), 6.76 (2H, d, J = 8.8 Hz, ArH-2′, 6′), 6.89 (2H, s, ArH-3″, 5″), 7.45 (2H, d, J = 8.8 Hz, ArH-3′, 5′), 7.62 (1H, s, ArH-3). MS m/z (%): 389 (M + 1, 100); HPLC purity: 98.3%.

6-(4-Cyano-2,6-dimethylphenoxy)-1-(4-cyanophenyl)-5-nitro-1*H*-benzoimidazole (39). Triethyl orthoformate (1 mL, excess) and HCl in diethyl ether (1N, 1 mL) were added successively to a solution of **37** (50 mg, 0.125 mmol) in DMF (3 mL) under N_2. The mixture was stirred at rt for 3 h, poured into water with pH adjusted to 6−7, and left to stand overnight. The resulting yellow solid was collected and washed with water. The crude product was purified by a silica gel column (eluent: CH_2Cl_2/EtOAc 10:1) to afford 42 mg of **39**, yield 88%, light-yellow solid, mp 250−252 °C. ^{1}H NMR ($CDCl_3$) δ ppm 2.21 (6H, s, 2 × CH_3), 6.43 (1H, s, ArH-7), 7.43 (2H, d, J = 8.8 Hz, ArH-3′, 5′), 7.46 (2H, s, ArH-3″, 5″), 7.86 (2H, d, J = 8.8 Hz, ArH-2′, 6′), 8.16

(1H, s, ArH-2), 8.54 (1H, s, ArH-4). MS m/z (%): 410 (M+1, 100). HPLC purity: 96.0%.

(4″-Cyano-2″,6″-dimethylphenoxy)-N^1-(4′-cyanophenyl)-4-nitrobenzene-1,2-diamine Hydrochloride (40). To a solution of **36** (100 mg) in acetone (10 mL) was slowly added HCl diethyl ether solution (18%, 3 mL), and a light-yellow solid appeared. The solid was filtered out and recrystallized from anhydrous MeOH to afford 52 mg of **40**, yield 48%, yellow solid, mp 170−171 °C. ^{1}H NMR δ ppm 2.07 (6H, s, 2 × CH_3), 6.17 (1H, s, ArH-6), 6.83 (2H, d, J = 8.8 Hz, ArH-2′, 6′), 7.40 (2H, s, ArH-3″, 5″), 7. 54 (1H, s, ArH-3), 7.56 (2H, d, J = 8.8 Hz, ArH-3′, 5′), 8.50 (1H, s, NH). MS m/z (%) 453 (M + 1, 100), 455 (M + 3, 100). HPLC purity: 97.6%.

HIV Growth Inhibition Assay in H9 Lymphocytes from Panacos, Inc. The evaluation of HIV-1 inhibition was carried out as follows according to established protocols. The human T-cell line, H9, was maintained in continuous culture with complete medium (RPMI 1640 with 10% fetal calf serum supplemented with L-glutamine at 5% CO_2 and 37 °C). Test samples were first dissolved in dimethyl sulfoxide at a concentration of 10 mg/mL to generate master stocks with dilutions made into tissue culture media to generate working stocks. The following drug concentrations were routinely used for screening: 100, 20, 4, and 0.8 μg/mL. For agents found to be active, additional dilutions were prepared for subsequent testing so that an accurate EC_{50} value could be determined. Test samples were prepared and to each sample well was added 90 μL of media containing H9 cells at 3 × 10^5 cells/mL and 45 μL of virus inoculum (HIV-1 IIIB isolate) containing 125 $TCID_{50}$. Control wells containing virus and cells only (no drug) and cells only (no virus or drug) were also prepared. A second set of samples were prepared identical to the first and were added to cells under identical conditions without virus (mock infection) for toxicity determinations (IC_{50} defined below). In addition, AZT was also assayed during each experiment as a positive drug control. On days 1 and 4 postinfection (PI), spent media was removed from each well and replaced with fresh media. On day 6 PI, the assay was terminated and culture supernatants were harvested for analysis of virus replication by p24 antigen capture. Compound toxicity was determined by XTT using the mock-infected samples.

Assay for Measuring the Inhibitory Activity of Compounds on HIV-1 IIIB Replication in MT-2 Cells. The inhibitory activity of compounds on HIV-1 IIIB replication was determined as previously described. In brief, 1 × 10^4 MT-2 cells were infected with an HIV-1 strain (100 $TCID_{50}$) in 200 μL of RPMI 1640 medium containing 10% FBS in the presence or absence of a test compound at graded concentrations overnight. Then, the culture supernatants were removed and fresh media containing no test compounds were added. On the fourth day postinfection, 100 μL of culture supernatants were collected from each well, mixed with equal volumes of 5% Triton X-100, and assayed for p24 antigen, which was quantitated by ELISA. Briefly, wells of polystyrene plates (Immulon 1B, Dynex Technology, Chantilly, VA) were coated with HIV immunoglobulin (HIVIG) in 0.085 M carbonate−bicarbonate buffer (pH 9.6) at 4 °C overnight, followed by washes with washing buffer (0.01 M PBS containing 0.05% Tween-20) and blocking with PBS containing 1% dry fat-free milk (Bio-Rad, Inc., Hercules, CA). Virus lysates were added to the wells and incubated at 37 °C for 1 h. After extensive washes, anti-p24 mAb (183−12H-5C), biotin-labeled antimouse IgG1 (Santa Cruz Biotechnology, Santa Cruz, CA), streptavidin-labeled horseradish peroxidase (Zymed, S. San Francisco, CA), and the substrate 3,3′,5,5′-tetramethylbenzidine (Sigma Chemical Co., St. Louis, MO) were added sequentially. Reactions were terminated by addition of 1N H_2SO_4. Absorbance at 450 nm was recorded in an ELISA reader (Ultra 386, TECAN, Research Triangle Park, NC). Recombinant protein p24 purchased from US Biological (Swampscott, MA) was included for establishing standard dose response curves. Each sample was tested in triplicate. The percentage of inhibition of p24 production was calculated as previously described.[25] The effective concentrations for 50% inhibition (EC_{50}) were calculated using a computer program, designated CalcuSyn,[26] kindly provided by Dr. T. C. Chou (Sloan-Kettering Cancer Center, New York, NY).

HIV-1 Infectivity Assay with Mutant Viral Strains in MT-2 Cell Line. A diluted drug resistant HIV-1 stock, mutated viral strain (8605MR or 6005MR from Panacos, Inc.), at a multiplicity of infection (MOI) of 0.001 $TCID_{50}$/cell was used to infect MT-2 cells. First, 20 μL of the virus and 20 μL of compounds at various concentrations in RPMI 1640 containing 10% fetal bovine serum were added to 20 μL of MT4 cells at 6 × 10^5 cells/mL in a 96-well microtiter plate. The cell/virus/compound mixture was then incubated at 37 °C in a humidified CO_2 incubator. Fresh medium (180 μL) containing an appropriate concentration of the compound was added to each well of the cultures on day 2. On day 4 postinfection, supernatant samples were harvested and assayed for P24 using an ELISA kit from ZeptoMetrix Corporation, Buffalo, NY.

Assessment of In Vitro Cytotoxicity in MT-2 Cells. The in vitro cytotoxicity of compounds on MT-2 cells was measured by XTT assay.[27] Briefly, 100 μL of the test compound at graded concentrations were added to equal volumes of cells (5 × 10^5/mL) in wells of a 96-well plate. After incubation at 37 °C for 4 days, 50 μL of XTT solution (1 mg/mL) containing 0.02 μM of phenazine methosulphate (PMS) was added. After 4 h, the absorbance at 450 nm was measured with an ELISA reader. The CC_{50} (concentration for 50% cytotoxicity) values were calculated using the CalcuSyn computer program as described above.

Assay for RT Enzymatic Inhibition. The RT activity of HIV-1_{DH012} (a primary isolate viral strain) was determined in the presence of various concentrations of the tested compounds using a Roche colorimetric HIV-1 RT assay kit following the protocol provided by the manufacturer.

Computational Study. Three-dimensional constructions of compounds **21**, **34**, and **37** were achieved by using the Sybyl version 7.2 software with the Tripos force-field and Gasteiger−Hückel atomic partial charges.[28] To get the correct orientation of the three compounds inside the HIV-1 RT enzyme, the constructions were made by modifying the experimental coordinates of the DAPY compound in the HIV-1 RT enzyme (PDB: 1s6q). Then the compounds were optimized with 20 simplex iterations followed by 1000 steps of Powell algorithm.

Energy minimizations were obtained with the Amber 9 software.[29] Ligand parameters were created according to the antechamber procedure and the partial charges were evaluated following the AM1 bond charge correction (AM1-BCC) method.[30−32] The general Amber force field[33] (gaff) was set for the ligand, whereas the ff03 force field[34] was used for the protein. Minimizations were done with 1000 steps of steepest descent followed by 4000 steps of conjugate gradient. Solvent effects were taken into account through general Born model implicit solvent model.[35−38] The molecular mechanics/general Born surface area (MM/GBSA) method[39−41] permitted the evaluation of the ligand−protein interaction free energies, and calculation details may be found elsewhere.[42] Finally, VMD software[43] was employed to visualize and analyze the 3D structures resulting from AMBER calculations.

Acknowledgment. We thank Nicole Kilgore at Panacos Pharmaceuticals, Inc., for providing data listed in Tables 1 and 2. HIV-1 mutated viral strains 8605MR (multimutated-RT: M41L, D67N, L210W, T215Y, M184 V, K103N) and 6005MR (multimutated-RT: M41L, L74 V, M184 V, L210W, T215Y, ins SS, A98G) were from Panacos, Inc., and HIV-1 strains IIIB, A17 were provided by the NIH AIDS Reagent and Reference Program, by contributions from Drs. R. Gallo, E. Emini, and Trimeris, Inc. This investigation was supported

by grants 20472114, 30930106, and 7052057 from the National Natural Science Foundation of China and Beijing government, respectively, awarded to L. Xie, as well as U.S. NIH grants awarded to K. H. Lee (AI33066), S. Jiang (AI46221), and C. H. Chen (AI65310).

Supporting Information Available: HPLC conditions and summary of HPLC purity data for final compounds. This material is available free of charge via the Internet at http://pubs.acs.org.

References

(1) Tantillo, C.; Ding, J. P.; Jacobo-Molina, A.; Nanni, R. G.; Boyer, P. L.; Hughes, S. H.; Pauwels, R.; Andries, K.; Janssen, P. A. J.; Arnold, E. Locations of anti-AIDS drug binding sites and resistance mutations in the three-dimensional structure of HIV-1 reverse transcriptase: implications for mechanisms of drug inhibition and resistance. *J. Mol. Biol.* **1994**, *243*, 369–387.

(2) Pauwels, R. New non-nucleoside reverse transcriptase inhibitors (NNRTIs) in development for the treatment of HIV infections. *Curr. Opin. Pharmacol.* **2004**, *4*, 437–446.

(3) Andries, K.; Azijn, H.; Thielemans, T.; Ludovici, D.; Kukla, M.; Heeres, J.; Janssen, P.; De Corte, B.; Vingerhoets, J.; Pauwels, R.; de Béthuneet, M. P. TMC125, a novel next- generation nonnucleoside reverse transcriptase inhibitor active against non-nucleoside reverse transcriptase inhibitor-resistant human immunodeficiency virus type 1. *Antimicrob. Agents Chemother.* **2004**, *48*, 4680–4686.

(4) Janssen, P. A. J.; Lewi, P. J.; Arnold, E.; Daeyaert, F.; de Jonge, M.; Heeres, J.; Koymans, L.; Vinkers, M.; Guillemont, J.; Pasquier, E.; Kukla, M.; Ludovici, D.; Andries, K.; de Bethune, M. P.; Pauwels, R.; Das, K.; Clark, A. D.; Frenkel, Y. V.; Hughes, S. H.; Medaer, B.; De Knaep, F.; Bohets, H.; De Clerck, F.; Lampo, A.; Williams, P.; Stoffels, P. In search of a novel anti-HIV drug: multidisciplinary coordination in the discovery of 4-[[4-[[4-[(1*E*)-2- cyanoethenyl]-2,6-dimethylphenyl] amino]-2-pyrimidinyl]amino]benzonitrile (R278474, rilpivirine). *J. Med. Chem.* **2005**, *48*, 1901–1909.

(5) De Clercq, E. Anti-HIV drugs: 25 compounds approved within 25 years after the discovery of HIV. *Int. J. Antimicrob. Agents* **2009**, *33*, 307–320.

(6) Tucker, T. J.; Sisko, J. T.; Tynebor, R. M.; Williams, T. M.; Felock, P. J.; Flynn, J. A.; Lai, M. T.; Liang, Y. X.; Gaughey, G. M.; Liu, M. Q.; Miller, M.; Moyer, G.; Munshi, V.; Perlow- Poehnelt, R.; Prasad, S.; Reid, J. C.; Sanchez, R.; Torrent, M.; Vacca, J. P.; Wan, B. L.; Yan, Y. W. Discovery of 3-{5-[(6-Amino-1*H*-pyrazolo [3,4-*b*]pyridine-3-yl)methoxy]-2- chlorophenoxy}-5-chlorobenzonitrile (MK-4965): a potent, orally bioavailable HIV-1 non-nucleoside reverse transcriptase inhibitor with improved potency against key mutant viruses. *J. Med. Chem.* **2008**, *51*, 6503–6511.

(7) Romines, K. R.; Freeman, G. A.; Schaller, L. T.; Cowan, J. R.; Gonzales, S. S.; Tidwell, J. H.; Andrews, C. W.; Stammers, D. K.; Hazen, R. J.; Ferris, R. G.; Short, S. A.; Chan, J. H.; Boone, L. R. Structure−activity relationship studies of novel benzophenones leading to the discovery of a potent, next generation HIV non-nucleoside reverse transcriptase inhibitor. *J. Med. Chem.* **2006**, *49*, 727–739.

(8) Himmel, D. M.; Das, K.; Clark, A. D.; Hughes, S. H.; Benjahad, A.; Oumouch, S.; Guillemont, J.; Coupa, S.; Poncelet, A.; Csoka, I.; Meyer, C.; Andries, K.; Nguyen, C. H.; Grierson, D. S.; Arnold, E. Crystal structures for HIV-1 reverse transcriptase in complexes with three pyridinone derivatives: a new class of non-nucleoside inhibitors effective against a broad range of drug-resistant strains. *J. Med. Chem.* **2005**, *48*, 7582–7591.

(9) Das, K.; Lewi, P. J.; Hughes, S. H.; Arnold, E. Crystallography and the design of anti-AIDS drugs: conformational flexibility and positional adaptability are important in the design of non-nucleoside HIV-1 reverse transcriptase inhibitors. *Prog. Biophys. Mol. Biol.* **2005**, *88*, 209–231.

(10) De Corte, B. L. From 4,5,6,7-Tetrahydro-5-methylimidazo[4,5,1-*jk*](1,4)benzodiazepin- 2(1*H*)-one (TIBO) to Etravirine (TMC125): Fifteen Years of Research on Non-Nucleoside Inhibitors of HIV-1 Reverse Transcriptase. *J. Med. Chem.* **2005**, *48*, 1689–1696.

(11) Das, K.; Clark, A. D., Jr.; Lewi, P. J.; Heeres, J.; De Jonge, M. R.; Koymans, L. M.; Vinkers, H. M.; Daeyaert, F.; Ludovici, D. W.; Kukla, M. J.; De Corte, B.; Kavash, R. W.; Ho, C. Y.; Ye, H.; Lichtenstein, M. A.; Andries, K.; Pauwels, R.; De Béthune, M.-P.; Boyer, P. L.; Clark, P.; Hughes, S. H.; Janssen, P. A.; Arnold, E. Roles of conformational and positional adaptability in structure based design of TMC125-R165335 (etravirine) and related non-nucleoside reverse transcriptase inhibitors that are highly potent and effective against wild-type and drug-resistant HIV-1 variants. *J. Med. Chem.* **2004**, *47*, 2550–2560.

(12) Das, K.; Bauman, J. D.; Clark, A. D.; Frenkel, Y. V.; Lewi, P. J.; Shatkin, A. J.; Hughes, S. H.; Arnold, E. High-resolution structures of HIV-1 reverse transcriptase/TMC278 complexes: strategic flexibility explains potency against resistance mutations. *Proc. Natl. Acad. Sci. U.S.A.* **2008**, *105*, 1466–1471.

(13) Heeres, J.; de Jonge, M.; Koymans, L. M. H.; Daeyaert, F. F. D.; Vinkers, M.; Van Aken, K. J. A.; Arnold, E.; Das, K.; Kilonda, A.; Hoornaert, G. J.; Compernolle, F.; Cegla, M.; Azzam, R. A.; Andries, K.; de Béthune, M.-P.; Azijn, H.; Pauwels, R.; Lewi, P. J.; Janssen, P. A. J. Design, synthesis, and SAR of a novel pyrazinone series with non-nucleoside HIV-1 reverse transcriptase inhibitory activity. *J. Med. Chem.* **2005**, *48*, 1910–1918.

(14) Zeevaart, J. G.; Wang, L.; Thakur, V. V.; Leung, C. S.; Tirado-Rives, J.; Bailey, C. M.; Domaoal, R. A.; Anderson, K. S.; Jorgensen, W. L. Optimization of azoles as anti-human immunodeficiency virus agents guided by free-energy calculations. *J. Am. Chem. Soc.* **2008**, *130*, 9492–9499.

(15) Sweeney, Z. K.; Dunn, J. P.; Li, Y.; Heilek, G.; Dunten, P.; Elworthy, T. R.; Han, X. C.; Harris, S. F.; Hirschfeld, D. R.; Hogg, J. H.; Huber, W.; Kaiser, A. C.; Kertesz, D. J.; Kim, W.; Mirzadegan, T.; Roepel, M. G.; Saito, Y. D.; Silva, T. M. P. C.; Swallow, S.; Tracy, J. L.; Villasenor, A.; Vora, H.; Zhou, A. S.; Klumpp, K. Discovery and optimization of pyridazinone non-nucleoside inhibitors of HIV-1 reverse transcriptase. *Bioorg. Med. Chem. Lett.* **2008**, *18*, 4352–4354.

(16) Frlan, R.; Kikelj, D. Recent progress in diaryl ether synthesis. *Synthesis* **2006**, *14*, 2271–2285.

(17) Li, F.; Wang, Q. R.; Ding, Z. B.; Tao, F. G. Microwave-assisted synthesis of diaryl ethers without catalyst. *Org. Lett.* **2003**, *5*, 2169–2171.

(18) Piersanti, G.; Giorgi, L.; Bartoccini, F.; Tarzia, G.; Minetti, P.; Gallo, G.; Giorgi, F.; Castorina, M.; Ghirardi, O.; Carminati, P. Synthesis of benzo[1,2-*d*;3,4-*d*]diimidazole and 1*H*-pyrazolo[4,3-*b*]pyridine as putative A2A receptor antagonists. *Org. Biomol. Chem.* **2007**, *5*, 2567–2571.

(19) Tian, X. T.; Qin, B. J.; Lu, H.; Lai, W. H.; Jiang, S.; Lee, K. H.; Chen, C. H.; Xie, L. Discovery of diarylpyridine derivatives as novel non-nucleoside HIV-1 reverse transcriptase inhibitors. *Bioorg. Med. Chem. Lett.* **2009**, *19*, 5482–5485.

(20) Gohlke, H.; Kiel, C.; Case, D. A. Insights into protein−protein binding by binding free energy calculation and free energy decomposition for the Ras−Raf and Ras−RalGDS complexes. *J. Mol. Biol.* **2003**, *330*, 891–913.

(21) Obiol-Pardo, C.; Rubio-Martinez, J. Comparative evaluation of MMPBSA and XSCORE to compute binding free energy in XIAP-peptide complexes. *J. Chem. Inf. Model.* **2007**, *47*, 134–142.

(22) Guimaraes, C. R.; Cardozo, M. MM-GB/SA rescoring of docking poses in structure-based lead optimization. *J. Chem. Inf. Model.* **2008**, *48*, 958–970.

(23) Ludovici, D. W.; De Corte, B. L.; Kukla, M. J.; Ye, H.; Ho, C. Y.; Lichtenstein, M. A.; Kavash, R. W.; Andries, K.; de Bethune, M. P.; Azijn, H.; Pauwels, R.; Lewi, P. J.; Heeres, J.; Koymans, L. M. H.; de Jonge, M. R.; Van Aken, K. J. A.; Daeyaert, F. F. D.; Das, K.; Arnold, E.; Janssen, P. A. J. Evolution of anti-HIV drug candidates. part 3: diarylpyrimidine (DAPY) analogues. *Bioorg. Med. Chem. Lett.* **2001**, *11*, 2235–2239.

(24) Mordant, C.; Schmitt, B.; Pasquier, E.; Demestre, C.; Queguiner, L.; Masungi, C.; Peeters, A.; Smeulders, L.; Bettens, E.; Hertogs, K.; Heeres, J.; Lewi, P.; Guillemont, J. Synthesis of novel diarylpyrimidine analogues of TMC278 and their antiviral activity against HIV-1 wild-type and mutant strains. *Eur. J. Med. Chem.* **2007**, *42*, 567–579.

(25) Zhao, Q.; Ma, L.; Jiang, S.; Lu, H.; Liu, S.; He, Y.; Strick, N.; Neamati, N.; Debnath, A. K. Identification of *N*-phenyl-*N*′-(2,2,6,6-tetramethylpiperidin-4-yl)-oxalamides as a new class of HIV-1 entry inhibitors that prevent gp120 binding to CD4. *Virology* **2005**, *339*, 213–225.

(26) Chou, T. C.; Talalay, P. Quantitative analysis of dose−effect relationships: the combined effects of multiple drugs or enzyme inhibitors. *Adv. Enzyme Regul.* **1984**, *22*, 27–55.

(27) Dupnik, K. M.; Gonzales, M. J.; Shafer, R. W. Most multidrug-resistant HIV-1 reverse transcriptase clones in plasma encode functional reverse transcriptase enzymes. *Antivir. Ther.* **2001**, *6*, 41–46.

(28) *SYBYL 7.0*; Tripos Inc.: 1699 South Hanley Road, St Louis, MO 63144.

(29) Case, D.; Darden, T.; Cheatham, T.; Simmerling, C.; Wang, J.; Duke, R.; Luo, R.; Merz, K.; Pearlman, D.; Crowley, M.; Walker, R.; Zhang, W.; Wang, B.; Hayik, S.; Roitberg, A.; Seabra, G.;

Wong, K.; Paesani, F.; Wu, X.; Brozell, S.; Tsui, V.; Gohlke, H.; Yang, L.; Tan, C.; Mongan, J.; Hornak, V.; Cui, G.; Beroza, P.; Mathews, D.; Schafmeister, C.; Ross, W.; Kollman, P. *AMBER, 9.0*; University of California: San Francisco, 2006.

(30) Dewar, M.; Zoebisch, E.; Healy, E.; Stewart, J. AM1: A new general purpose quantum mechanical molecular model. *J. Am. Chem. Soc.* **1985**, *107*, 3902–3909.

(31) Jakalian, A.; Bush, B. L.; Jack, D. B.; Bayly, C. I. Fast, efficient generation of high-quality atomic charges. AM1-BCC model: I. Method. *J. Comput. Chem.* **2000**, *21*, 132–146.

(32) Jakalian, A.; Jack, D. B.; Bayly, C. I. Fast, efficient generation of high-quality atomic charges. AM1-BCC model: II. Parameterization and validation. *J. Comput. Chem.* **2002**, *23*, 1623–1641.

(33) Wang, J.; Wolf, R. M.; Caldwell, J. W.; Kollman, P. A.; Case, D. A. Development and testing of a general amber force field. *J. Comput. Chem.* **2004**, *25*, 1157–1174.

(34) Duan, Y.; Wu, C.; Chowdhury, S.; Lee, M. C.; Xiong, G.; Zhang, W.; Yang, R.; Cieplak, P.; Luo, R.; Lee, T.; Caldwell, J.; Wang, J.; Kollman, P. A point-charge force field for molecular mechanics simulations of proteins based on condensed-phase quantum mechanical calculations. *J. Comput. Chem.* **2003**, *24*, 1999–2012.

(35) Beroza, P.; Case, D. Calculations of proton-binding thermodynamics in proteins. *Methods Enzymol.* **1998**, *295*, 170–189.

(36) Cramer, C. J.; Truhlar, D. G. Implicit solvation models: equilibria, structure, spectra, and dynamics. *Chem. Rev.* **1999**, *99*, 2161–2200.

(37) Gilson, M. K. Theory of electrostatic interactions in macromolecules. *Curr. Opin. Struct. Biol.* **1995**, *5*, 216–223.

(38) Madura, J. D.; Davis, M. E.; Gilson, M. K.; Wade, R. C.; Luty, B. A.; Mc Cammon, J. A. Biological applications of electrostatic calculations and brownian dynamics simulations. *Rev. Comput. Chem.* **1994**, *5*, 229–267.

(39) Kollman, P. A.; Massova, I.; Reyes, C.; Kuhn, B.; Huo, S.; Chong, L.; Lee, M.; Lee, T.; Duan, Y.; Wang, W.; Donini, O.; Cieplak, P.; Srinivasan, J.; Case, D. A.; Cheatham, T. E., III. Calculating structures and free energies of complex molecules: combining molecular mechanics and continuum models. *Acc. Chem. Res.* **2000**, *33*, 889–897.

(40) Wang, J.; Morin, P.; Wang, W.; Kollman, P. A. Use of MM-PBSA in reproducing the binding free energies to HIV-1 RT of TIBO derivatives and predicting the binding mode to HIV-1 RT of efavirenz by docking and MM-PBSA. *J. Am. Chem. Soc.* **2001**, *123*, 5221–5230.

(41) Wang, W.; Kollman, P. A. Computational study of protein specificity: the molecular basis of HIV-1 protease drug resistance. *Proc. Natl. Acad. Sci. U.S.A.* **2001**, *98*, 14937–14942.

(42) Luo, Y.; Barbault, F.; Gourmala, C.; Zhang, Y.; Maurel, F.; Hu, Y.; Fan, B. Cellular interaction through LewisX cluster: theoretical studies. *J. Mol. Model.* **2008**, *14*, 901–910.

(43) Humphrey, W.; Dalke, A.; Schulten, K. VMD—visual molecular dynamics. *J. Mol. Graphics* **1996**, *14*, 33–38.